Adsorption of Au and Pd Atoms on Thin SiO_2 Films: the Role of Atomic Structure

M. Baron, D. Stacchiola, S. Ulrich, N. Nilius, S. Shaikhutdinov,* and H.-J. Freund

Fritz-Haber Institut der Max-Planck Gesellschaft, Department of Chemical Physics, Faradayweg 4-6, D-14195 Berlin, Germany

U. Martinez, L. Giordano, and G. Pacchioni*

Dipartimento di Scienza dei Materiali, Università di Milano-Bicocca, Via R. Cozzi, 53−20125, Milano, Italy

Received: September 12, 2007; In Final Form: December 11, 2007

The low-temperature deposition of Au and Pd atoms on thin SiO_2 films grown on Mo(112) has been studied by scanning tunneling microscopy (STM), infrared reflection absorption spectroscopy, and CO adsorption. On the monolayer films, gold forms three-dimensional nanoparticles at temperatures as low as 10 K and does not affect the phonon spectra of the silica films. On the other hand, palladium exhibits structure-dependent behavior. Pd deposition leads to a red-shift of the phonon frequency of the monolayer and not of the multilayer films. The amount of CO that may adsorb on the Pd particles formed on the "O-poor" monolayer films is much smaller than that on the "O-rich" films (with an additional O-layer on the Mo surface) and multilayer films. These experimental findings have been rationalized on the basis of density functional theory calculations showing that the Pd atoms penetrate into the hexagonal rings of the silica network and bind at the SiO_2/Mo interface, which in turn depends on the atomic structure of the film. This bonding is very strong on the O-poor films so that Pd is unable to bind CO, while on the O-rich films CO may even pull out the Pd atoms from the interface thus promoting aggregation and particle formation. The Pd migration into the film has been directly supported by low-temperature STM images.

1. Introduction

In the past few years the study of ultrathin oxide films grown on metal substrates has attracted the interest of the surface chemistry community because of the discovery that these systems, under particular circumstances, can behave in a different way with respect to the corresponding surfaces of bulk oxides.[1−7] When the thickness of the oxide film is in the range of a few atomic layers, the interaction with the metal substrate, together with structural and morphological changes, can lead to completely different chemistry with respect to the thicker films and to new and unprecedented phenomena. Examples pointing in this direction have been reported for films of MgO,[2−6] FeO,[7] and alumina.[5] For instance, gold atoms or clusters deposited on 2−3 layers thick MgO/Ag(100) films become negatively charged. This effect has dramatic consequences on the structure and shape of the supported clusters, which form two-dimensional structures, while on thicker films they form three-dimensional particles.[3,6] Modulation of the work function of a FeO/Pt(111) film provides the basis for using these supports to induce spatial ordering and self-assembling of supported nanoparticles;[7] unusual one-dimensional gold nanostructures can be formed and stabilized on ultrathin alumina layers grown on NiAl substrates,[5] etc. These few examples well illustrate the potential of ultrathin films in the design of new materials with largely unexplored properties in catalysis but also in fields such as molecular electronics and sensors.

While several oxides in the form of thin films have been studied for more than a decade, intense efforts have only recently been directed toward silica. It has been shown that thin silica films grow amorphous on Mo(110) and Mo(100) substrates,[8,9] but well-ordered crystalline silica films can be prepared on a Mo(112) substrate.[10,11] The SiO_2/Mo(112) films have been used to study the deposition of small metal clusters with the aim to design accurate models of supported metal catalysts,[12−20] but the atomic structure of the film has been the subject of an intense debate.[21−27]

Our data show that the SiO_2/Mo(112) film consists of a single layer of SiO_4 tetrahedra which share three oxygen atoms forming three Si−O−Si linkages, with the fourth oxygen directly bound to the Mo substrate.[23,26] This structure corresponds to a two-dimensional film with a honeycomb-like structure. In addition, the SiO_2/Mo(112) surface prepared under oxygen-rich conditions results in a new phase where a layer of oxygen atoms is adsorbed only on the Mo surface, i.e., below the silica layer.[28] Thus, two kinds of silica films can be prepared on the Mo(112) substrate: one with additional O atoms at the interface, referred to as "O-rich" to discriminate it from the "O-poor" film without these atoms. The two phases exhibit slightly different values of the phonon frequency, which is basically related to the Si−O stretching mode. The experimental and theoretical arguments in favor of the continuous hexagonal film have been summarized in a recent comprehensive paper.[29]

The possibility of preparing well-defined, crystalline SiO_2/Mo(112) films opened new perspectives for the study, interpretation, and theoretical modeling of the deposition of metal atoms and clusters. In a recent theoretical study we have considered the adsorption of Pd and Au isolated atoms on the O-poor SiO_2/Mo(112) films.[19] We found that Au atoms interact very weakly with the silica surface, and a high mobility on the surface is therefore expected even at very low temperatures. In the minimum energy configuration, the Au atom is sitting above

* Corresponding authors. E-mail: gianfranco.pacchioni@unimib.it (G.P.), shamil@fhi-berlin.mpg.de (S.S.).

10.1021/jp077326f CCC: $40.75
Published on Web 02/12/2008

the center of a six-membered ring, but the binding energy (ca. 0.1 eV) is extremely low. In principle, the Au atoms could bind much more strongly (by about 2 eV) at the interface between the silica film and the Mo(112) substrate. The calculations showed, however, that this kind of interstitial gold is quite difficult to form since the barrier for migration into the film amounts to about 0.9 eV.[19] This means that when the temperature of the substrate is raised, the Au atoms will either desorb from the surface or aggregate to form small particles before diffusion into the film sets in. Of course, the scenario may be different in the presence of surface defects. On the SiO_2/Mo(112) films there are domain boundaries running in the [−110] direction where alternating eight- and four-membered rings are present, and the Au atoms can penetrate into these defects. Furthermore, it has been shown theoretically that point defects at the surface of silica films bind gold quite strongly.[20]

The calculations predicted a completely different behavior for Pd. First, a Pd single atom interacts much stronger than Au with the Si and O atoms of the film, with binding energies of about 0.3−0.4 eV. However, more interesting is that the Pd atom can easily penetrate into the film (the barrier is very small, if any) and become bound to the Mo atoms, with a binding energy of 3.30 eV.[19] On the basis of these results, quite different behavior is expected for the Pd and Au atoms deposited onto the SiO_2/Mo(112) films.

In order to verify this hypothesis, here we report on the comparative study of the Pd and Au atom deposition on the O-poor and O-rich monolayer films as well as on a multilayer silica film, used as a reference support. Concomitantly, the density functional theory (DFT) calculations are extended to the O-rich films and also to the adsorption of CO on both films. The experimental results provide compelling evidence for the structural models proposed by DFT. This represents an interesting example for the close interplay between structural and adsorption properties, where a small change in the structure of the oxide−metal interface may result in quite substantial differences in adsorption phenomena.

2. Experimental and Computational Details

2.1. Experiments. The experiments were performed in an ultrahigh vacuum (UHV) chamber (base pressure below 1×10^{-10} mbar) equipped with scanning tunneling microscopy (STM), X-ray photoelectron spectroscopy, an infrared reflection absorption spectroscopy (IRAS), and standard facilities for sample preparation. The IRAS spectra were measured with p-polarized light at 84° grazing angle of incidence (resolution ~4 cm^{-1}). The STM images were obtained in a separate UHV chamber equipped with a home-built microscope operated at liquid helium temperatures.

The preparation of the monolayer silica films has been described in details elsewhere.[23,29] Briefly, the clean Mo(112) surface was exposed to 5×10^{-8} mbar of O_2 at 900 K for 5 min, followed by the deposition of ca. 1.2 monolayer (ML) of Si at the same oxygen pressure and temperature. Subsequent annealing at 1200 K in UHV or 10^{-6} mbar O_2 leads to the formation of O-poor and O-rich silica films, respectively.[28]

Multilayer silica films were grown by deposition of >3 ML of Si in UHV onto clean Mo(112) at 300 K followed by oxidation at 400 K in 5×10^{-7} mbar of O_2. The sample was then slowly heated to 900 K in 5×10^{-7} mbar of O_2 and finally annealed at 1150 K in UHV.[30]

Pd and Au (both 99.99%, Goodfellow) were vapor deposited at ~90 K (and ~10 K for the STM measurements) using a commercial evaporator (Focus EFM 3) with a deposition rate of ca. 0.2 Å/min. For each Pd/silica sample, a new silica film was prepared. The Pd coverage is presented in the text as the nominal thickness (in Å); approximately 2.3 Å corresponds to a monolayer coverage.

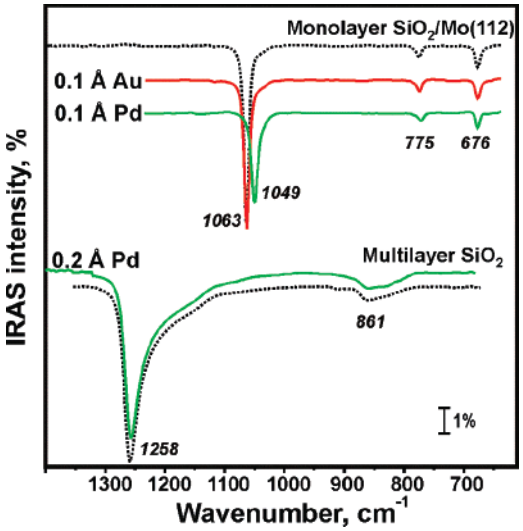

Figure 1. Phonon region of the IRA spectra obtained on an O-poor monolayer SiO_2/Mo(112) film and on a multilayer silica film, exposed to small amounts of Au and Pd as indicated (see the text). The spectra for the clean silica surfaces are shown for comparison (dotted lines). The spectra are offset for clarity.

2.2. Calculations. The calculations are based on DFT at the level of the generalized gradient approximation (using the PW91 exchange-correlation functionals[31]). The method is implemented in the *VASP* program[32,33] which uses a plane-wave basis set (with a kinetic energy cutoff at 400 eV). The electron−ion interactions are described by the projector augmented wave method (PAW).[34] The Mo(112) substrate has been modeled by seven Mo layers which well reproduce the band structure of bulk Mo.[21] The O atom linking the SiO_4 tetrahedra to the Mo surface is in a bridge position over two protruding Mo atoms.[23] During geometry optimization, the three Mo bottom layers were frozen at bulk positions while the top four layers were optimized. The atoms within the slab are relaxed until the atomic forces are less than 0.01 eV/Å.

The surface stoichiometry of the slab that gives a Mo(112)-c(2 × 2) structure is $Mo_{14}Si_2O_5$, as observed by low-energy electron diffraction. For modeling the adsorption of Au or Pd atoms, the cell size has been increased to (4 × 2) in order to represent a low concentration of adsorbed species. The calculations have been done in a 2 × 2 × 1 grid of *k* points. The surface slabs are separated by a vacuum gap of 10 Å.

3. Results and Discussion

Figure 1 shows the IRA spectrum of an O-poor silica film with the main feature at 1063 cm^{-1} assigned to the Si−O−Mo asymmetric stretching vibrations.[22,23,35] It has been previously shown that for the O-rich films this mode shifts to the lower frequencies by ~10 cm^{-1}.[28] All these features, i.e., at 1063 cm^{-1} for O-poor and at 1049 cm^{-1} for O-rich phases as well as the weak bands at ~775 and 675 cm^{-1}, were reproduced by DFT calculations.[28]

Infrared spectroscopy serves to study the impact of the admetals on the oxide phonons.[36] The deposition of 0.1 Å of Pd causes a 14 cm^{-1} red-shift of the Si−O−Mo stretching band and signal broadening as shown in Figure 1. For comparison, incorporation of Al into the film to produce aluminosilicate films results in a ~30 cm^{-1} red-shift.[37] The red-shift is Pd-coverage-

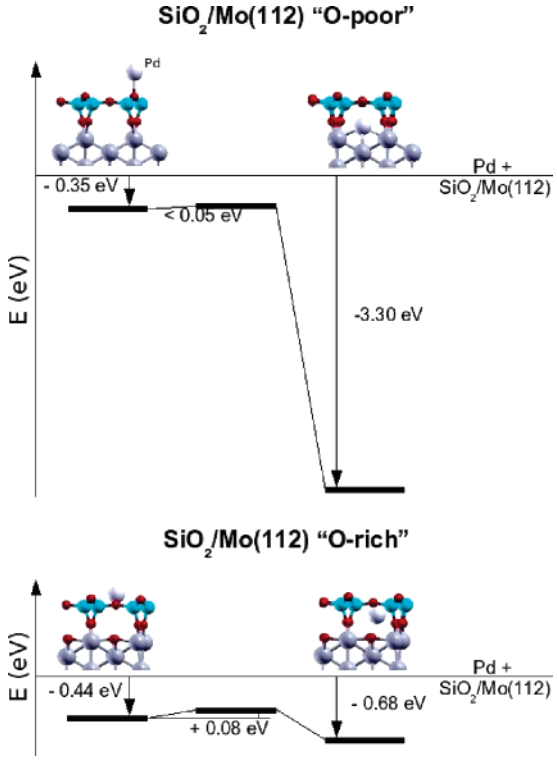

Figure 2. Energy profile of the interaction of a single Pd atom with an O-poor (top) and O-rich (bottom) SiO_2/Mo(112) film. The central panel indicates the energy of the transition state. The side view of the silica film and the position of the Pd adatom in the structure are shown. Color key: large gray spheres, Mo; white spheres, Pd; small blue spheres, Si; red spheres, O.

dependent, as observed for alumina films, and various mechanisms have been proposed to explain this behavior.[36] The adsorption of Pd on the O-rich films showed a similar effect (not shown here). In contrast, the deposition of the same amount of Au only decreases the intensity but does not induce any peak shift on both O-poor and O-rich films.

To study the effect of the film thickness on the interaction with metal atoms, we also deposited Pd onto the atomically flat, amorphous SiO_2 films of approximately three monolayers in thickness (henceforth referred to as "multilayer" film).[30] Even for subnanometer thickness, these films show phonon vibrations at 1258 cm^{-1} characteristic of the bulk SiO_2 systems.[38] Figure 1 shows that the silica phonon in the multilayer film is not affected by the adsorption of even larger amounts of Pd. The observation of the spectral shift for the Pd and not for the Au deposition is a first indication of the different interaction of these two metals with the monolayer silica films. Furthermore, the fact that Pd adsorption on a thicker silica film does not modify the phonon spectrum implies a specific adsorption behavior of Pd on the monolayer films.

Figure 2 shows the interaction energy profile obtained from DFT calculations for a Pd atom bound to monolayer SiO_2/Mo(112) films. On the O-rich phase, the Pd atom sits above the center of the ring and is bound by 0.44 eV. A small energy barrier (0.08 eV) separates this local minimum from a deeper minimum where the Pd atom is adsorbed below the silica layer with a binding energy of 0.68 eV. The effect of penetration of the Pd atom below the silica layer is much more dramatic on the O-poor phase: the estimated barrier for diffusion is negligible, and the binding at the interface is very large, ca. 3.3 eV.[19] In this case, the Pd atom interacts directly with the Mo metal surface, while on the O-rich phase this is hampered by the presence of the adsorbed O atom (see Figure 2). In both

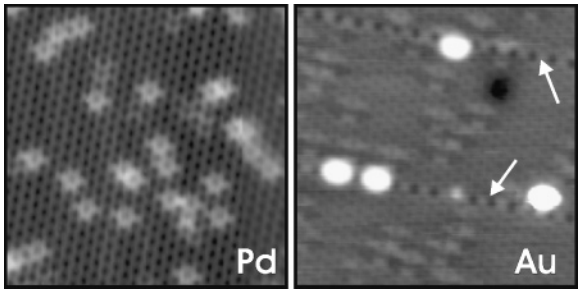

Figure 3. Low-temperature STM images (14 × 14 nm^2) of Pd (left) and Au (right) deposited onto the O-poor SiO_2/Mo(112) monolayer films at ~10 K. The arrows mark antiphase domain boundaries. The tunneling parameters are (a) sample bias 1.75 V, current 0.05 nA; (b) 1.25 V, 0.05 nA.

cases, however, the presence of the Pd atom at the interface slightly perturbs the structure of the silica film and affects the phonon spectrum. In particular, the calculations show that the main phonon frequency is red-shifted by 11 cm^{-1} for the O-poor (from 1058 to 1047 cm^{-1}) and by 23 cm^{-1} for the O-rich structures (from 1043 to 1020 cm^{-1}), respectively, which is consistent with the experimental findings.

The adsorption of Au is predicted to be completely different. According to the calculations, Au atoms do not migrate into the rings because of very weak interaction with the O-poor film and the large atomic size, giving rise to a higher barrier than that for Pd. On the O-rich phase, subsurface Au is even unbound. Given the low binding energy of Au with the silica surface of about 0.1 eV, a very low diffusion barrier is expected, so that surface diffusion and subsequent aggregation of Au adatoms likely occurs at low temperatures.

This hypothesis on Pd and not Au migration into the film is fully supported by a low-temperature STM study. Figure 3 shows STM images of the O-poor silica films possessing small amounts of Pd and Au as deposited at 10 K. The honeycomb-like structure of the silica surface and also antiphase domain boundaries are clearly resolved in these images. The Au deposition results in the formation of small Au clusters in the vicinity of the line defects. In line with theoretical predictions, the Au atoms impinging on the surface have sufficient kinetic energy to diffuse across the surface and find the defect sites where they bind strongly. The interaction of Au adatoms with the regular surface is so weak that even at ~10 K no isolated Au atoms were observed on the terraces.

In contrast, STM images of Pd deposits revealed some randomly located spots, such as six-fold stars, which appear much brighter than the surrounding areas. No features are present in these images, which could be associated with the Pd atoms located on top of the silica surface. Therefore, the STM study provides strong evidence for the diffusion of the Pd atoms through the silica film to the SiO_2/Mo(112) interface. These Pd atoms perturb the electronic structure of the silica film, thus leading to a different image contrast.

Concomitantly, one can expect that the different interaction of Pd with the silica films will manifest itself in the adsorption of CO as a probe molecule, since CO adsorption on the Pd surfaces is well understood and a large database exists for IR spectra.[39]

Two bands in the CO stretching region were observed at 90 K at saturation CO coverage. One is around 2105 cm^{-1} assigned to terminal CO, and another broad feature is centered at ~1950 cm^{-1}, which is assigned to multicoordinated CO molecules (e.g., see inset in Figure 4).

Figure 4 plots the integral peak area as a function of the amount of Pd deposited. (Note that the same trend is found

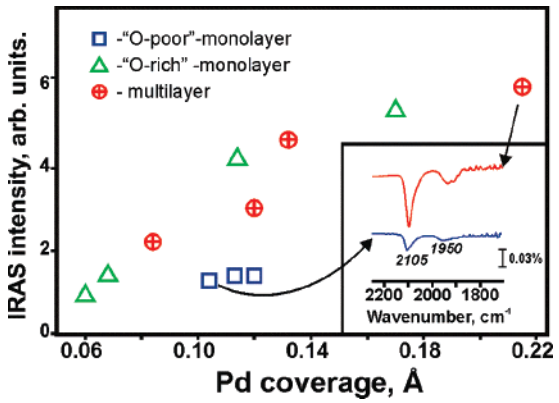

Figure 4. Integral area of CO IRAS signal (2200−1800 cm^{-1}) as a function of Pd coverage measured on different silica films, as indicated. The inset shows the IR spectra observed for the samples, marked by the arrows, after exposure to 20 L of CO at 90 K.

separately for either terminal or multicoordinated CO bands.) Although the intensity of the IR lines of adsorbed CO is not linearly proportional to the site population, it provides a qualitative measure of the total CO uptake and hence the Pd surface area. Data show that Pd atoms on the O-rich monolayer and the multilayer films behave similarly, while Pd atoms on the O-poor films exhibit much lower CO adsorption capacity than those on the O-rich films. In principle, there may have two reasons for this. It can be due to different Pd dispersions (particle size and density) that result in different metal surface areas on these two silica surfaces. Alternatively, some portion of Pd is not accessible to CO as a result of migration into the film.

To better understand the microscopic aspects of the observed behavior, we have performed DFT calculations on the CO adsorption. On the O-poor phase, where Pd is strongly bound to the substrate, CO is unbound to Pd (by 0.11 eV). Even if we assume that a Pd−CO complex is formed under elevated CO pressures, the barrier to pull the Pd−CO species out from the hexagonal ring would be very large, approximately 1.7 eV (see Figure 5). This means that on the O-poor surface, CO is unable to bind to the Pd atoms, which are trapped at the interface. The situation changes on the O-rich film. Here CO binds strongly (by 1.04 eV) to Pd atoms located in the "cavity". The formation of a strong Pd−CO bond weakens the interaction of Pd with the substrate so that the Pd−CO complex becomes unbound by 0.69 eV and can easily escape from the cavities by overcoming a barrier of 0.23 eV only. On the surface, the Pd−CO complex is bound to the silica layer by 0.66 eV and can diffuse and eventually aggregate with other Pd atoms or clusters. Thus, CO adsorption has a completely different effect on Pd atoms deposited on O-poor or O-rich silica monolayers. This may explain recent observation of CO-induced sintering effect on the low-temperature Pd deposition.[18]

4. Summary

The combined experimental and theoretical study of the interaction of Pd and Au atoms with monolayer and multilayer silica films demonstrates the importance of structural details in determining of the adsorption properties of oxide surfaces. In particular, Au behaves in a similar way on all three silica supports considered, namely, O-rich and O-poor monolayer films and three-monolayers amorphous films. Gold aggregates at the surface preferentially on the line defects. In contrast, the Pd interaction with the oxide film and its tendency to bind CO are substrate-dependent. On the monolayer films, this manifests

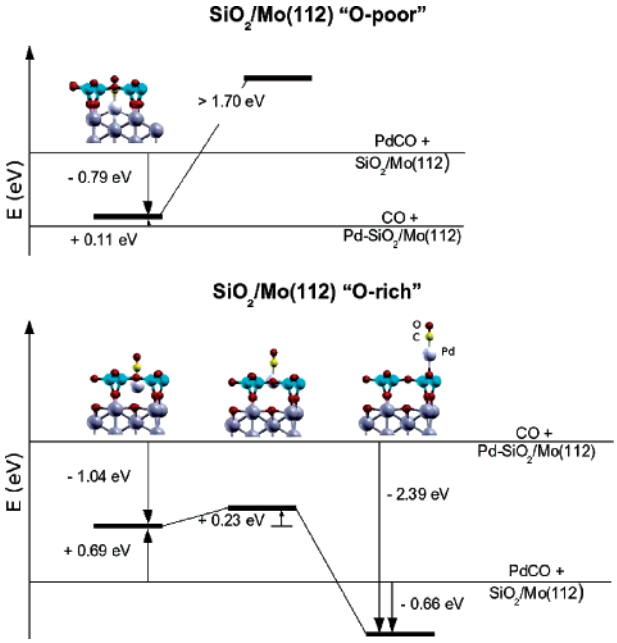

Figure 5. Energy profile of the interaction of CO with a Pd atom adsorbed on O-poor (top) and O-rich (bottom) phases of SiO_2/Mo-(112). The central panel indicates the transition state between initial and final configurations. The insets show the structure of the silica film (side view) and the position of the PdCO complex in the subsurface state (left) and above the surface (right). Color key: large gray spheres, Mo; white spheres, Pd; small blue spheres, Si; red spheres, O.

itself in a change of the phonon frequency and the bright appearance of the six-membered silica rings in the STM images due to the presence of subsurface Pd atoms, confirming previous theoretical predictions that Pd can migrate into the six-membered rings.[19] It was also found that the CO uptake for Pd deposited on O-poor films is much smaller than that on the O-rich phase and multilayer silica.

DFT calculations showed that on the O-poor films the Pd atoms strongly bind at the silica−Mo interface and do not interact with CO, so that the total amount of adsorbed CO molecules remains small. On the O-rich monolayer film, the Pd atoms are also adsorbed subsurface, but the CO is able to form stable PdCO complexes which can escape from the cavity and aggregate to form Pd nanoparticles. In contrast, Au does not show any of these effects because the size of the rings is too small for penetration to occur. The adatoms bind only weakly on the surface and can easily diffuse and aggregate on the silica surfaces. The continuous silica monolayer can therefore be viewed as the first example of a two-dimensional sieve, which could be used to selectively permit diffusion of metal atoms or small molecules to a metal substrate.

Acknowledgment. The work has been supported by the European STREP project GSOMEN and by the COST Action D41 "Inorganic oxides: surfaces and interfaces". Part of the computing time was provided by the Barcelona Supercomputing Center—Centro Nacional de Supercomputación (BSC-CNS).

References and Notes

(1) Freund, H. J. *Surf. Sci.* **2007**, *601*, 1438.
(2) Pacchioni, G.; Giordano, L.; Baistrocchi, M. *Phys. Rev. Lett.* **2005**, *94*, 226104.
(3) Ricci, D.; Bongiorno, A.; Pacchioni, G.; Landman, U. *Phys. Rev. Lett.* **2006**, *97*, 036106.
(4) Sterrer, M.; Risse, T.; Martinez Pozzoni, U.; Giordano, L.; Heyde, M.; Rust, H.-P.; Pacchioni, G.; Freund, H.-J. *Phys. Rev. Lett.* **2007**, *98*, 096107.

(5) Kulawik, M.; Nilius, N.; Freund, H. J. *Phys. Rev. Lett.* **2006**, *96*, 036103.
(6) Sterrer, M.; Risse, T.; Heyde, M.; Rust, H. P.; Freund, H. J. *Phys. Rev. Lett.* **2007**, *98*, 206103
(7) Nilius, N.; Rienks, E. D. L.; Rust, H. P.; Freund, H. J. *Phys. Rev. Lett.* **2005**, *95*, 066101.
(8) Xe, X.; Goodman, D. W. *Surf. Sci.* **1993**, *282*, 323.
(9) He, J. W.; Xu, X.; Corneille, J. S.; Goodman, D. W. *Surf. Sci.* **1992**, *279*, *119* (1992).
(10) Schroeder, T.; Adelt, M.; Richter, B.; Naschitzki, M.; Bäumer, M.; Freund, H.-J. *Surf. Rev. Lett.* **2000**, *7*, 7.
(11) Schroeder, T.; Giorgi, J. B.; Bäumer, M.; Freund, H.-J. *Phys. Rev. B: Condens. Matter Mater. Phys.* **2002**, *66*, 165422.
(12) Ozensoy, E.; Min, B. K.; Santra, A. K.; Goodman, D. W. *J. Phys. Chem. B* **2004**, *108*, 4351.
(13) Kim, Y. D.; Wei, T.; Wendt, S.; Goodman, D. W. *Langmuir* **2003**, *19*, 7929.
(14) Wallace, W. T.; Min, B. K.; Goodman, D. W. *J. Mol. Catal. A: Chem.* **2005**, *228*, 3.
(15) Chen, M. S.; Goodman, D. W. *Surf. Sci.* **2005**, *574*, 259.
(16) Min, B. K.; Wallace, W. T.; Goodman, D. W. *J. Phys. Chem. B* **2004**, *108*, 14609.
(17) Giorgi, J. B.; Schroeder, T.; Bäumer, M.; Freund, H. J. *Surf. Sci.* **2002**, *498*, L71.
(18) Lu, J. L.; Kaya, S.; Weissenrieder, J.; Gao, H.-J.; Shaikhutdinov, S.; Freund, H.-J. *Surf. Sci.* **2006**, *600*, L153.
(19) Giordano, L.; Del Vitto, A.; Pacchioni, G. *J. Chem. Phys.* **2006**, *124*, 034701.
(20) Martinez, U.; Giordano, L.; Pacchioni, G. *J. Phys. Chem. B* **2006**, *110*, 17015.
(21) Ricci, D.; Pacchioni, G. *Phys. Rev. B: Condens. Matter Mater. Phys.* **2004**, *69*, 161307.
(22) Chen, M. S.; Santra, A. K.; Goodman, D. W. *Phys. Rev. B: Condens. Matter Mater. Phys.* **2004**, *69*, 155404.
(23) Weissenrieder, J.; Kaya, S.; Lu, J. L.; Gao, H. J.; Shaikhutdinov, S.; Freund, H. J.; Sierka, M.; Todorova, T. K.; Sauer, J. *Phys. Rev. Lett.* **2005**, *95*, 076103.
(24) Todorova, T. K.; Sierka, M.; Sauer, J.; Kaya, S.; Weissenrieder, J.; Lu, J. L.; Gao, H. J.; Shaikhutdinov, S.; Freund, H.-J. *Phys. Rev. B: Condens. Matter Mater. Phys.* **2006**, *73*, 165414.
(25) Chen, M.; Goodman, D. W. *Surf. Sci.* **2006**, *600*, L255.
(26) Giordano, L.; Ricci, D.; Pacchioni, G.; Ugliengo, P. *Surf. Sci.* **2005**, *584*, 225.
(27) Giordano, L.; Ricci, D.; Pacchioni, G.; Ugliengo, P. *Surf. Sci.* **2007**, *601*, 588.
(28) Sierka, M.; Todorova, T. K.; Kaya, S.; Stacchiola, D.; Weissenrieder, J.; Lu, J.; Gao, H.; Shaikhutdinov, S.; Freund, H.-J.; Sauer, J. *Chem. Phys. Lett.* **2006**, *115*, 424.
(29) Kaya, S.; Baron, M.; Stacchiola, D.; Weissenrieder, J.; Shaikhutdinov, S.; Todorova, T. K.; Sierka, M.; Sauer, J.; Freund, H.-J. *Surf. Sci.* **2007**, *601*, 4849.
(30) Stacchiola, D.; Baron, M.; Kaya, S.; Weissenrieder, J.; Shaikhutdinov, S.; Freund, H.-J. *Appl. Phys. Lett.* **2008**, *92*, 011911.
(31) Perdew, J. P.; Chevary, J. A.; Vosko, S. H.; Jackson, K. A.; Pederson, M. R.; Singh, D. J.; Fiolhais, C. *Phys. Rev. B: Condens. Matter Mater. Phys.* **1992**, *46*, 6671.
(32) Kresse, G.; Hafner, J. *Phys. Rev. B: Condens. Matter Mater. Phys.* **1993**, *47*, 558.
(33) Kresse, G.; Furthmüller, J. *Phys. Rev. B: Condens. Matter Mater. Phys.* **1996**, *54*, 11169.
(34) Blöchl, P. E. *Phys. Rev. B: Condens. Matter Mater. Phys.* **1994**, *50*, 17953.
(35) Wendt, S.; Ozensoy, E.; Wei, T.; Frerichs, M.; Cai, Y.; Chen, M. S.; Goodman, D. W. *Phys. Rev. B: Condens. Matter Mater. Phys.* **2005**, *72*, 115409.
(36) Frank, M.; Wolter, K.; Magg, N.; Heemeier, M.; Kühnemuth, R.; Bäumer, M.; Freund, H.-J. *Surf. Sci.* **2001**, *492*, 270.
(37) Stacchiola, D.; Kaya, S.; Weissenrieder, J.; Kuhlenbeck, H.; Shaikhutdinov, S.; Freund, H.-J.; Sierka, M.; Todorova, T. K.; Sauer, J. *Angew. Chem.* **2006**, *45*, 7636.
(38) Kirk, C. T. *Phys. Rev. B: Condens. Matter Mater. Phys.* **1988**, *38*, 1255.
(39) Hollins, P. *Surf. Sci. Rep.* **1992**, *16*, 51.